ELSEVIER

Materials Science and Engineering B 129 (2006) 193–199

ENGINEERING B

www.elsevier.com/locate/mseb

Preparation and characterization of Fe_2O_3–TiO_2 thin films on glass substrate for photocatalytic applications

E. Celik [a], A.Y. Yildiz [a], N.F. Ak Azem [a], M. Tanoglu [b], M. Toparli [a,*], O.F. Emrullahoglu [c], I. Ozdemir [a]

[a] *Dokuz Eylul University, Faculty of Engineering, Department of Metallurgical and Materials Engineering, Bornova, Izmir 35100, Turkey*
[b] *Izmir Institute of Technology, Faculty of Engineering, Department of Mechanical Engineering, Urla, 35437 Izmir, Turkey*
[c] *Afyon Kocatepe University, Faculty of Engineering, Department of Ceramic Engineering, 03200 Afyon, Turkey*

Received 9 November 2005; received in revised form 19 January 2006; accepted 20 January 2006

Abstract

Fe_2O_3–TiO_2 coatings were successfully prepared on glass slide substrates using sol–gel method for photocatalytic applications. The phase structure, thermal, microstructure and surface properties of the coatings were extensively characterized by using X-ray diffractometry (XRD), differential thermal analysis/thermogravimetry (DTA/TG), scanning electron microscopy (SEM) and atomic force microscopy (AFM). Their adhesion and absorbance properties were investigated by a scratch tester and UV–vis spectroscopy. Four different solutions were prepared by changing Fe/Ti molar ratios. Glass substrates were coated by solutions of Ti-alkoxide, Fe-chloride, glaciel acetic acid and isopropanol. The obtained gel films were dried at 300 °C for 10 min and subsequently heat-treated at 500 °C for 5 min in air. The oxide thin films were annealed at 600 °C for 60 min in air. The influence of Fe^{3+} concentration and number of layers on structure of the films was established. In addition, XRD results revealed that Fe_2O_3–TiO_2 films composed of TiO_2, $Fe_2Ti_3O_9$, Ti_3O_5 and Fe_3O_4 phases. According to DTA/TG result, it was determined that endothermic and exothermic reactions were formed at temperatures between 80 and 650 °C due to solvent removal, combustion of carbon based materials and oxidation of Fe and Ti. SEM observations exhibited that the coating structure becomes more homogeneous depending on an increase of Fe/Ti molar ratios and thus a regular surface morphology forms with increasing Fe/Ti ratio. It was also seen that as the Fe/Ti ratio increases the surface roughness of the films increases. Critical adhesion force of thin films with Fe/Ti ratio of 0, 0.07, 0.18 and 0.73 were found to be 9, 25, 28 and 21 mN, respectively. The methylene blue solutions photocatalyzed by TiO_2 based thin films shows characteristic absorption bands at 420 nm.

Keywords: Fe_2O_3–TiO_2 coatings; Sol–gel; Photocatalytic activity

1. Introduction

Titania (TiO_2) with wide bandgap semiconductor has recently attracted much attention because of its large surface area and pores, which are of great importance in photocatalysis, highly specific chemical sensors, luminescence, self-cleaning surfaces, carbon nanotubes and solar cells [1,2]. Notably, TiO_2 is one of the most widely used photocatalysts due to its high photocatalytic efficiency and thermostability. In recent years, much research has been made on the utilization of TiO_2 powders in photodegrading various organic pollutants in water. The ways to improve the catalytic properties of TiO_2 have also attracted much attention [3].

Many organic compounds can be decomposed in aqueous solution in the presence of TiO_2 powders or coatings illuminated with near UV or sunlight. When TiO_2 is irradiated by UV rays, pairs of electrical charges-holes are created in the valency band and electrons in the conductivity band. The holes react with water molecules or with the hydroxyl ions and hydroxyl radicals are formed, which are strong oxidants of the organic molecules. It has been shown that the photocatalytic activity of TiO_2 is influenced by the crystal structure (anatase and rutile), surface area, size distribution, porosity, surface hydroxyl group density, etc. These properties have an influence on the production of electron–hole pairs on the surface adsorption and desorption processes as well as the redox process [4]. However, a disadvantage of TiO_2 is that the bandgap energy is approximately

* Corresponding author. Tel.: +90 232 388 2880/17; fax: +90 232 388 78 64.
E-mail address: mustafa.toparli@deu.edu.tr (M. Toparli).
URL: http://www.deu.edu.tr.

0921-5107/$ – see front matter © 2006 Elsevier B.V. All rights reserved.
doi:10.1016/j.mseb.2006.01.013

3.2 eV; therefore UV illumination is necessary to photoactivate this semiconductor. Another disadvantage of TiO_2 is that charge carrier recombination occurs within nanoseconds and, in absence of promoters (e.g. Pt or RuO_2), the photocatalytic activity is low. A wide range of metal ions, in particular transition metal ions (iron, chromium, copper, vanadium and cobalt), have been used as dopants for TiO_2 [4]. Of these metal ions, ferric ion (Fe^{3+}) with UV radiation on the decomposition of organic compounds has an important effect. The role of ferric ion on the decomposition of alachlor is placed in the increase of the concentration of $^{\bullet}OH$ in solution, namely the enhancement of the decomposition rate.

With an increasing amount of chemical contaminants such as pesticides and fertilizers in a water stream, wastewater treatment of environmental endocrine disruptors has become an important issue of a worldwide concern. Herbicides such as alachlor has been classified as a carcinogen and has been known as a highly toxic endocrine disruptor, where the allowed maximum concentration is 0.002 mg/l.

Several methods to remove toxic and organic compounds in wastewater, including alachlor, have been reported recently. Various chemical derivatives from alachlor were found in the groundwater sampled from the cornfield. It was reported that the degradation kinetics of alachlor dissolved in water by the photocatalysis in the presence of both $FeCl_3$ and TiO_2 followed the first order kinetics with a short half life in the range of 10–17 min. Recently, the photocatalytic decomposition of xenobiotic organics using TiO_2 has attracted much attention as a promising method in water purification. The system of TiO_2/UV has been known to have many important advantages in the water purification. With the photocatalytic oxidation process, a number of organic compounds dissolved or dispersed in water can be efficiently mineralized. Furthermore, TiO_2 as a photocatalyst is inexpensive and can be easily recycled on a technical scale [5,6].

TiO_2 thin films can be prepared on the substrate by various techniques such as chemical vapor deposition, chemical spray pyrolysis, electrodeposition and sol–gel method [7]. The sol–gel process is suitable for producing composite materials of high purity without multiple steps. In addition to this, the sol–gel process offers new approaches to the synthesis of oxide materials. One unique property of the sol–gel process is the ability to go all the way from the molecular precursor to the product, allowing a better control of the whole process and the synthesis of tailor made materials (monolithic gels, fibers, films and powders) for various applications [8].

In this work, we report preparation and characterization of Fe_2O_3–TiO_2 thin films on glass slide substrate by using four different solutions of Ti-alkoxide, Fe-chloride, glaciel acetic acid and isopropanol via sol–gel process. The phase structure, thermal, microstructure and surface properties of the coatings were characterized using X-ray diffractometry (XRD), differential thermal analysis/thermograviometry (DTA/TG), scanning electron microscopy (SEM) and atomic force microscopy (AFM). The adhesion properties of coatings were investigated by scratch tester. Absorption spectra of reaction products of methylene blue solutions photocatalyzed by TiO_2 based thin films on glass substrate were determined by UV–vis absorption spectroscopy.

2. Experimental procedure

Fe_2O_3–TiO_2 films were synthesized with solutions which were prepared as follows: the precursors were weighted out in fume hood and iron chloride ($FeCl_3{\cdot}6H_2O$) powder were dissolved in isopropanol and glaciel acetic acid. Titanium isopropoxide was incorporated into the mixture. Then the prepared solutions were stirred for 1 h in an open vessel kept at room temperature in air in order to yield a clear and homogeneous solution (see Fig. 1). Four different solutions were prepared by changing Fe/Ti ratios such as 0, 0.007, 0.18 and 0.73. After preparation of transparent solutions, pH values of the transparent solutions were measured to determine their acidic and basic characteristics using a standard pH meter with Mettler Tolede electrode.

Prior to the coating process, glass slide substrates with dimension of 15 mm × 15 mm × 3 mm were ultrasonically cleaned in acetone. The solutions were deposited on glass slide substrates. The solution temperature was kept at 25 °C during the deposition. The glass substrates were coated by solutions of Ti-alkoxide, Fe-chloride, glaciel acetic acid and isopropanol. The deposited gel films were dried at 300 °C for 10 min and subsequently heat-treated at 500 °C for 5 min in air. We repeated six cyclics of this film-making process. The thick multilayered films were annealed at 600 °C for 60 min in air to make them polycrystalline. XRD patterns of thin films were determined by means of a Rigaku diffractometer with a Cu Kα irradiation (wavelength, λ = 0.15418 nm). Thermal behaviour of Fe–Ti based powder, which was dried at 300 °C for 5 h in air, was evaluated by using DTA/TG machine. Surface roughnesses of Fe_2O_3–TiO_2

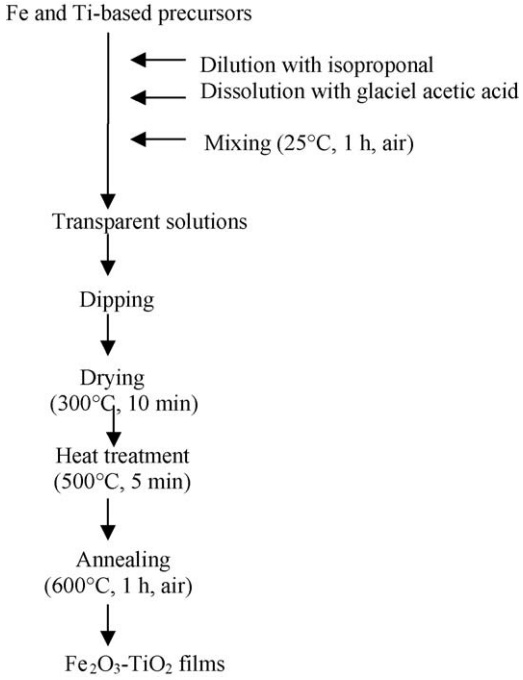

Fig. 1. Flow chart of sol–gel processing for Fe_2O_3–TiO_2 films.

thin films on glass substrate were characterized via AFM with model, Digital Instruments III-A. The surface topographies of Fe_2O_3–TiO_2 films were examined by using SEM (JEOL JSM 6060). Adhesion strength of the films was measured by a Shimadzu Scanning Scracth Tester SST-W101. UV–vis absorption spectra of reaction products of methylene blue solutions photocatalyzed by TiO_2 based thin films on glass substrate were recorded by a Perkin-Elmer double beam scanning spectrophotometer.

3. Results and discussion

Fig. 2 demonstrates pH values of the solutions depending on Fe/Ti molar ratios. According to this result, it is clear that acidity of the solutions increases due to the fact that $FeCl_3{\cdot}6H_2O$ precursor possesses the content of Cl ions as Fe/Ti ratio increases. That is to say, pH values of the solutions with Fe/Ti molar ratios of 0.07, 0.18 and 0.73 were found to be 2.4, 1.5 and 0.6, respectively. Inasmuch as pH value of the solution is an important factor influencing the formation of the polymeric three-dimensional structure of the gel during the gelation process, it should be taken into consideration while preparing solutions. While ramified structure is randomly formed in acidic conditions, separated clusters are formed from the solutions showing basic characters [9]. The other factor is dilution of the solution using solvent. The excess solvent physically affects the structure of the gel, because the liquid phase during the aging procedures mainly consists of the excess solvent. The changes in the gel structure at this stage partly influence the structure of the final film [10].

The phase identification of Fe_2O_3–TiO_2 films on glass slide substrates was performed by means of XRD techniques after annealing process at 600 °C for 1 h in air. The results are given in Fig. 3, where one observes the evolution of the X-ray diffraction profiles as a function of the Fe/Ti molar ratios. Amourphous and anatase structures were found because the gel coated samples were heat-treated in the temperature range of 300 and 600 °C. Especially, anatase phase of TiO_2 having tetragonal structure was strongly observed at 600 °C as explained in Refs. [11,12]. It can be seen that the peaks at 2θ of 25.28, 38.08, 44.52, 47.92, 53.32 and 62.66 are assigned to (1 0 1), (0 0 4), (1 1 2), (2 0 0), (1 0 6) and (2 1 5) lattice planes of TiO_2. Additional peaks including $Fe_2Ti_3O_9$, Ti_3O_5 and Fe_3O_4 were found as well as TiO_2 anatase phase because of Fe additives. In Fe doped TiO_2 having 0.07 and 0.18 ratios, $Fe_2Ti_3O_9$ and Ti_3O_5 phases were determined as additional peaks. In addition to these, Fe_3O_4 phase was only found in Fe_2O_3–TiO_2 films with 0.73 ratio.

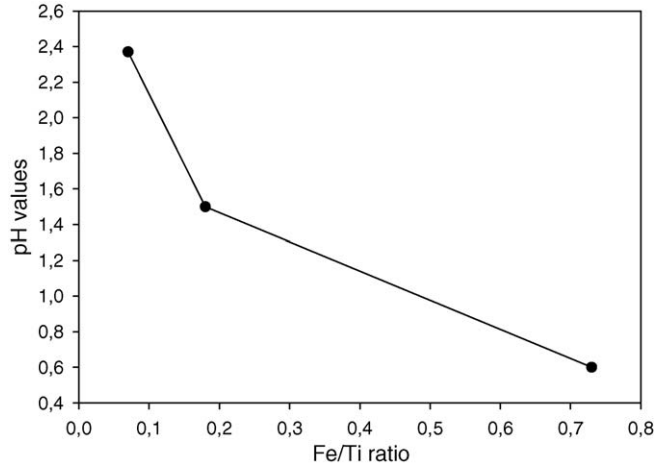

Fig. 2. pH values of the solutions depending on Fe/Ti ratio.

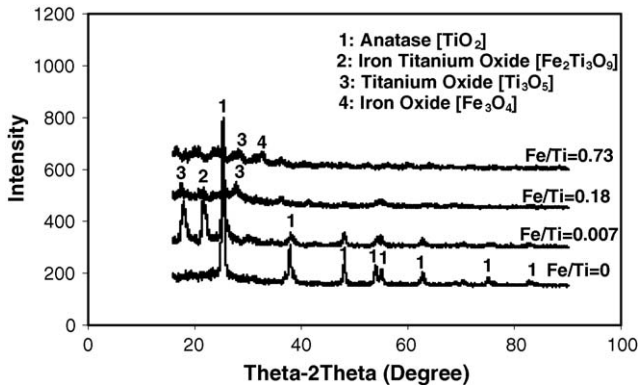

Fig. 3. XRD patterns of Fe_2O_3–TiO_2 thin films produced on glass substrate depending on Fe/Ti ratios (a) 0, (b) 0.07, (c) 0.18 and (d) 0.73.

Thermal behaviour of Fe–Ti based powders dried at 300 °C for 5 h in air is depicted in Fig. 4. DTA curve revealed that endothermic and exothermic reactions became at temperatures between 80 and 450 °C due to the fact that physical water and solvent in the gel evaporated and carbon based materials coming from alkoxide, solvent and chelating agent burnt out. The first thermal phenomenon was the solvent removal at temperature of approximately 125 °C. At this temperature, the endothermic reaction is mostly owing to evaporation of volatile organic components. The second phenomenon was combustion of OR groups at temperatures between 250 and 450 °C. A large great exothermic peak was determined at this temperature range owing to combustion of carbon based materials. The last stage was the formation of ceramic oxides between 450 and 650 °C. Upon investigated TG curve, weight loss of the powder was determined to be 26% and weight loss continued until 650 °C. While percentage of the weight loss was 24 % until 500 °C, this value was decreased to 2% at the temperature range of 500 and 650 °C.

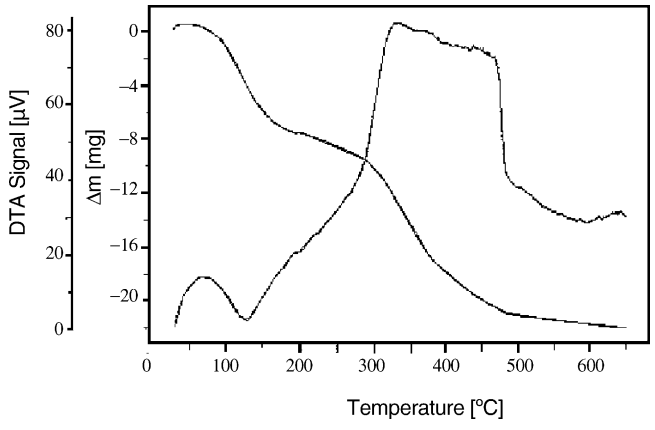

Fig. 4. DTA–TG curves of Fe–Ti based powder which was dried at 300 °C for 5 h in air.

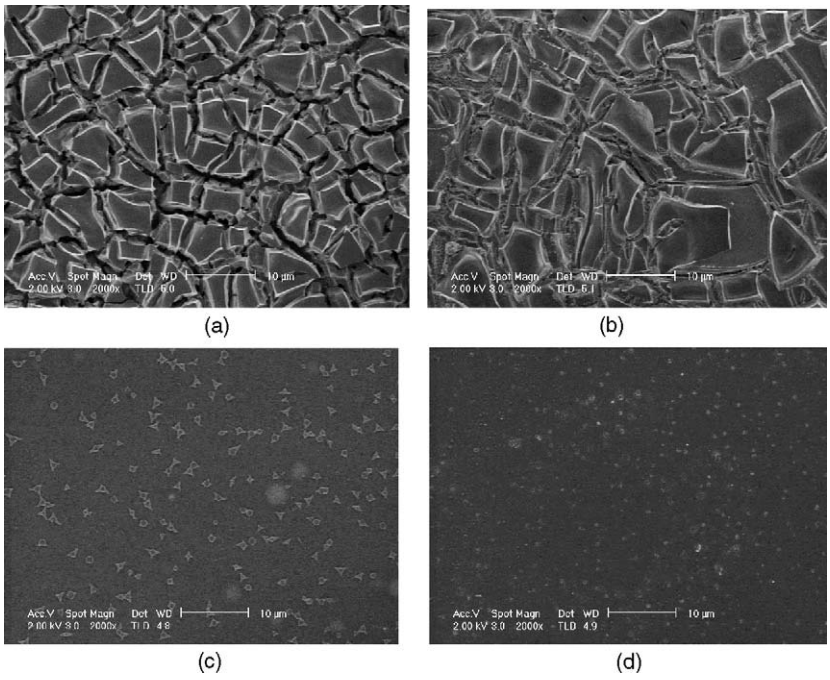

Fig. 5. SEM micrographs of Fe_2O_3–TiO_2 films on glass substrate including Fe/Ti ratios such as (a) 0, (b) 0.07, (c) 0.18 and (d) 0.73. Number of layer is 6. The scale bars are 10 μm.

Fig. 5 shows SEM micrographs of Fe_2O_3–TiO_2 films on glass slide substrate with different Fe/Ti ratios. In order to increase the amount of calcinations for TiO_2, the process should be carried out at a high temperature which is approved in Fig. 5a. The microstructure of the coating showed in Fig. 5b reveals some pores throughout the coating. As shown in Fig. 4c, the defects formed during production stage increases with increasing coating thickness due to the lack of wettability. In sum, as the amount of Fe/Ti ratio increases the coating structure becomes more homogeneous. The application of thermal processes carried out at high temperatures results in some cracks inside the coating, however, coating layers did not flake off (see Fig. 5d).

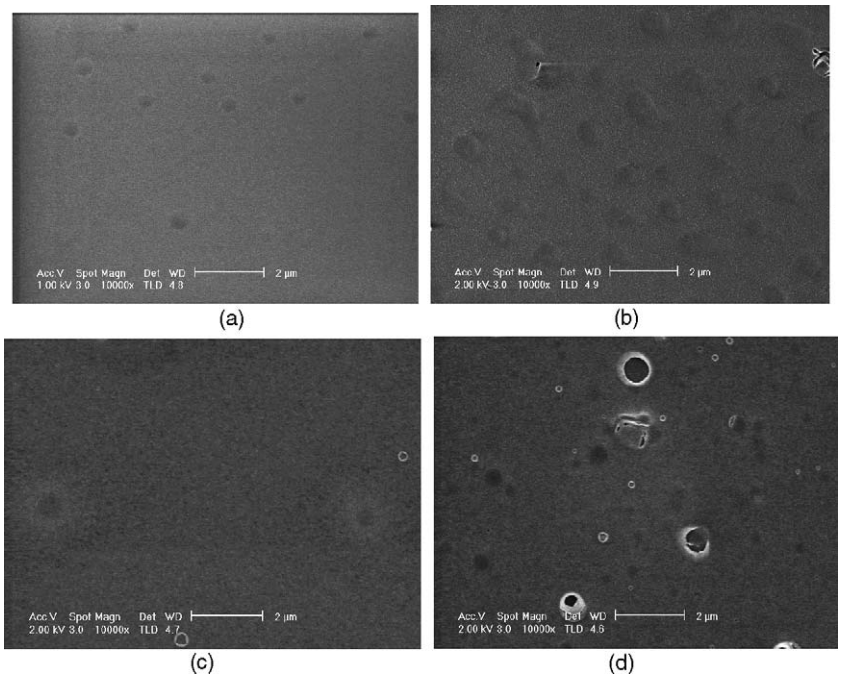

Fig. 6. SEM micrographs of Fe_2O_3–TiO_2 films on glass substrate with different number of layers. The numbers of layer are (a) 1, (b) 3, (c) 5 and (d) 6. The scale bars are 2 μm.

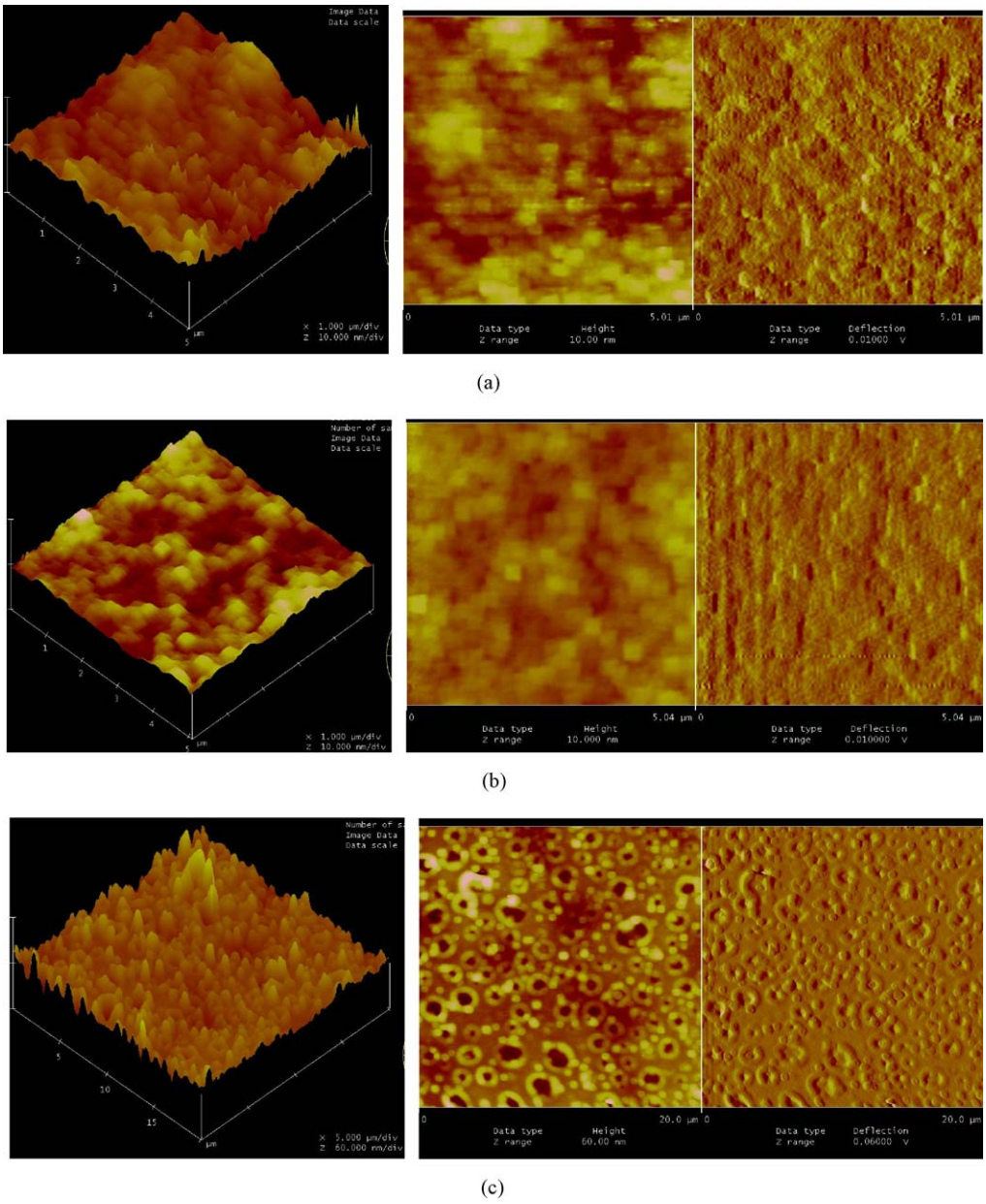

Fig. 7. AFM micrographs of Fe_2O_3–TiO_2 films prepared in different Fe/Ti ratios such as (a) 0.07, (b) 0.18 and (c) 0.73. The pictures on the left are AFM angle view images and the pictures on the right are AFM top view images.

Fig. 6 denotes SEM micrographs of Fe_2O_3–TiO_2 films on glass substrate having different layers. As shown from microstructural observations, a regular surface morphology forms as Fe/Ti ratio increases. Thin films are obtained for the coatings which contain few layers. The film thickness and surface defects increase in accordance with number of layers. However, more pores and homogeneous structure could be obtained by changing viscosity of the solutions.

AFM two- and three-dimensional images of Fe_2O_3–TiO_2 films deposited on glass substrate are shown in Fig. 7. The surface morphologies of Fe_2O_3–TiO_2 films are obviously different. It is noted that as the Fe/Ti molar ratio increases the surface roughness of the films exhibited an increase.

The aim of scratch test is to evaluate the adhesion between coating and substrate. In the test, increasing normal load is applied to the diamond stylus. Simultaneously, diamond stylus is scratched over the surface of the coating with a constant speed. The load at which failure occurs on the coating is defined as critical load. The test load versus cartridge output (%) curves for TiO_2 based films on glass substrates are given in Fig. 8. During the scratch test, with increasing applied load, friction of the stylus becomes high, therefore delay in movement of the stylus from that of the cartridge body also becomes large. This delay is given as a cartridge output [13]. Critical load values of the TiO_2 coatings were found from Fig. 8, when sudden increase takes place at the cartridge output. As can be seen in Table 1, critical

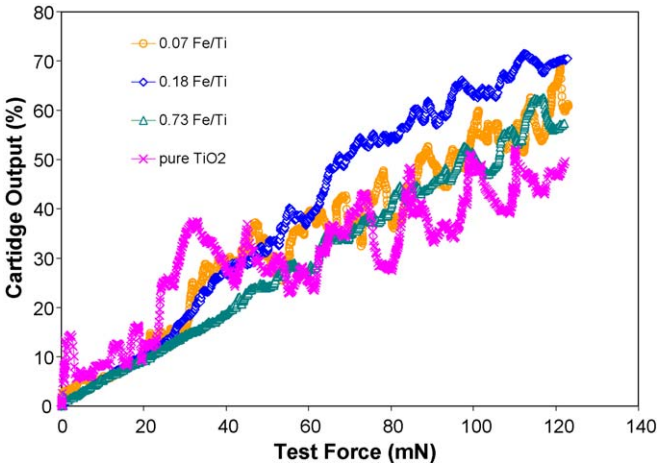

Fig. 8. Cartridge percentage–test force curves for Fe_2O_3–TiO_2 films with different Fe/Ti ratios.

Table 1
Critical load values of the coatings

Coating	Critical load (mN)
Pure TiO_2	9
0.07 Fe/Ti	25
0.18 Fe/Ti	28
0.73 Fe/Ti	21

load values of Fe/Ti molar ratio with 0, 0.07, 0.18 and 0.73 for thin films were found to be 9, 25, 28 and 21 mN, respectively. Among these coatings, the coating with 0.18 Fe/Ti ratio shows better adhesion strength to the glass substrate among the other coatings.

The activity of the thin film catalyst was determined by photo-oxidation of methylene blue. In Fig. 9 depicts UV–vis spectra of reaction product of methylene blue solution photocatalyzed by thin films of Fe_2O_3–TiO_2 and TiO_2 on glass substrate after UV irradiation of sample. The solutions including methylene blue show characteristic absorption bands at 420 nm. In

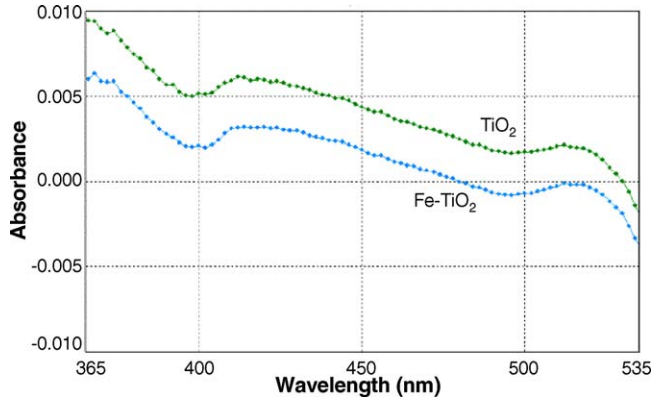

Fig. 9. UV–vis spectra of reaction product of methylene blue solution photocatalyzed by a thin film of Fe_2O_3–TiO_2 on glass substrate after UV irradiation of sample. The blue curve is Fe_2O_3–TiO_2 and the green curve is TiO_2. (For interpretation of the references to colour in this figure legend, the reader is referred to the web version of the article.)

order to improve the photocatalytic efficiency of TiO_2, reducing recombination of photo-generated electrons and holes, it has been observed that some certain metal ions doping can enhance photocatalytic activity of TiO_2 [14–16]. It has been shown that different percentages of Fe^{3+} ions doped TiO_2 showed improvement over TiO_2 by extending the wavelength of TiO_2 from UV to the visible region. Based on UV–vis results, the additive of Fe, the foreign metal ions, on the surface of TiO_2 surface increases the photocatalytic activity of anatase which is ascribed to the inhibiting electron–hole pair recombination and enhancing interfacial charge transfer reactions.

4. Conclusion

Fe_2O_3–TiO_2 thin films were synthesized on glass substrate from different solutions of Ti-alkoxide, Fe-chloride, glaciel acetic acid and isopropanol via sol–gel process for photocatalytic applications. The results can be summarized as follows:

(1) The acidity of the solutions increases due to the fact that $FeCl_3{\cdot}6H_2O$ precursor possesses Cl ions as Fe/Ti ratio increases.
(2) The TiO_2, $Fe_2Ti_3O_9$, Ti_3O_5 and Fe_3O_4 phases were found from the films.
(3) The endothermic and exothermic reactions were formed at temperatures between 80 and 650 °C due to solvent removal, combustion of carbon based materials and oxidation of Fe and Ti. Weight loss of the powder was determined to be 26% and weight loss continued until 650 °C.
(4) The coating structure becomes more homogeneous and a regular surface morphology forms with increasing Fe/Ti ratio.
(5) The film thickness and surface defects increase with number of layers. As the Fe/Ti molar ratio increases the surface roughness of the films increases.
(6) Critical load values of Fe/Ti molar ratio with 0, 0.07, 0.18 and 0.73 for thin films were found to be 9, 25, 28 and 21 mN, respectively.
(7) The solutions including methylene blue show characteristic absorption bands at 420 nm.

References

[1] C. Wang, Q. Li, R.-D. Wang, Mater. Lett. 58 (2004) 1424–1426.
[2] A. Brioude, P. Vincent, C. Journet, J.C. Plenet, S.T. Purcell, Appl. Surf. Sci. 22 (2004) 4–9.
[3] G. Colón, M.C. Hidalgo, M. Macías, J.A. Navío, J.M. Doña, Appl. Catal. B: Environ. 43 (2003) 163–173.
[4] C.C. Trapalis, P. Keivanidis, G. Kordas, M. Zaharescu, M. Crisan, A. Szatvanyi, M. Gartner, Thin Solid Films 433 (2003) 186–190.
[5] C.S. Ryu, M.-S. Kim, B.-W. Kim, Chemosphere 53 (2003) 765–771.
[6] Y.S. Choi, B.W. Kim, J. Chem. Technol. Biotechnol. 75 (2000) 1145–1150.
[7] Y.U. Ahn, E.J. Kim, H.T. Kim, S.H. Hahn, Mater. Lett. 57 (2003) 4660–4666.
[8] W.-M. Liu, Y.-X. Chen, G.-T. Kou, T. Xu, D.C. Sun, Wear 254 (2003) 994–1000.
[9] A.C. Pierre, Introduction to Sol–Gel Processing, Kluwer Academic Publishers, 1998, p. 25.

[10] F. Dumeignil, K. Sato, M. Imamura, N. Matsubayashi, E. Payen, H. Shimada, Appl. Catal. A: Gen. 241 (2003) 319–329.
[11] W.-P. Tai, J.-H. Oh, Thin Solid Films 422 (2002) 220–224.
[12] J.C. Yu, H.Y. Tang, J. Yu, H.C. Chan, L. Zhang, Y. Xie, H. Wang, S.P. Wang, J. Photochem. Photobiol. A: Chem. 153 (2002) 211–219.
[13] Instruction Manual, Shimadzu Scanning Scratch Tester SST-W101. Shimadzu Corporation, 2002.
[14] W. Choi, J. Phys. Chem. 98 (1994) 13669–13679.
[15] C.C. Trapalis, P. Keivanidis, G. Kordas, M. Zaharescu, M. Crisan, A. Szatvanyi, M. Gartner, Thin Solid Films 433 (2003) 186–190.
[16] J.-C. Xu, Y.-L. Shi, J.-E. Huang, B. Wang, H.-L. Li, J. Mol. Catal. A: Chem. 219 (2004) 351–355.